Synthesis and Characterization of Zincosilicates with the SOD Topology

Miguel A. Camblor,[†] Raul F. Lobo, Hubert Koller, and Mark E. Davis*

Chemical Engineering, California Institute of Technology, Pasadena, California 91125

Received June 29, 1994. Revised Manuscript Received September 2, 1994[®]

The incorporation of Zn^{2+} into tetrahedral framework positions of zeolites with the sodalite topology (SOD) is obtained by direct synthesis. The zincosilicates are characterized by thermal analyses, a Rietveld refinement of powder X-ray diffraction (XRD) data, and infrared (IR) and ^1H, ^{23}Na, ^{13}C, and ^{29}Si MAS NMR spectroscopies. A zinc substitution level as high as Si/Zn = 6–7 is achieved and constitutes by far the largest extent of isomorphous substitution by a doubly charged heteroatom in the framework of a zeolite. Two types of β-cage occupancies (TMA^+ and Na^+) are observed.

Introduction

The preparation of zeolites with isomorphous substitutions of Al and/or Si by other tri- or tetravalent elements in tetrahedral positions (T) is a field of active research that has led to new ion exchangers and catalysts.[1] In addition to synthesizing known zeolites with new chemical compositions, the presence of heteroatoms in the synthesis mixture can yield molecular sieves with new topologies. The crystallization of new materials by inclusion of heteroatoms into silicate gels has been demonstrated with the divalent heteroatoms Be^{2+} and Zn^{2+}. Unlike aluminosilicates, beryllo- and zincosilicates frequently display topologies that contain rings comprised of three tetrahedra (3MR), e.g., beryllosilicate Lovdarite[2] and zincosilicate VPI-7.[3] This type of ring has very small TOT angles (~130°) that are relatively unstable in pure-silicate or aluminosilicate frameworks. The only example of a zeolite with 3MR is ZSM-18.[4] ZSM-18 is synthesized using a very specific template and the presence of 3MR's in the structure is most likely a direct consequence of the templating organic cation.[4]

It has been hypothesized that to synthesize new silica-based microporous solids with lower framework densities (FD) a MINR parameter (the size of the smallest ring to which all the T atoms belong) lower than 4 is necessary.[5] Thus, the ability of Be^{2+} and Zn^{2+} to promote the formation of 3MR in silicate frameworks may allow the synthesis of new low FD materials provided an adequate "template" can be used to stabilize the void spaces in the framework. This strategy raises the question of whether it is possible to "template" the synthesis of a structure in which there are two negative charges per framework heteroatom that thus requires the presence of two countercations (at least one of them presumably voluminous) in close proximity to one another. The term "to template" is used here in a loose sense to refer to the filling of the void spaces of a zeolite by the bulky organic cations frequently used as structure-directing or structure-stabilizing agents.

Although a number of phosphate microporous materials containing divalent elements (Zn^{2+}, Be^{2+}, Co^{2+}, ...)[6,7] have been prepared (a single charge is introduced in the framework per divalent element in this case) none of the known 3MR containing microporous beryllosilicates or zincosilicates, with the exception of the high-silica VPI-8,[8–10] has been synthesized with an organic structure-directing molecule that resides within the void space of the crystal. Moreover, it has been previously reported that in the hydrothermal synthesis of microporous zincosilicates, the inorganic cation is the main factor determining the nature of the phase formed (Na^+ for VPI-7, Li^+ for VPI-8, K^+ for VPI-9 and VPI-10, Rb^+ for VPI-9 or Zn-analcime, and Cs^+ for Zn-analcime).[9,10]

If the extensive substitution of Al^{3+} by a doubly charged cation such as Zn^{2+} in the framework of low-silica zeolites is feasible, the synthesis of materials with a cation-exchange capacity in excess of those presently available or with special cation-exchange selectivities might be possible. These new types of ion exchangers could have a large technological impact. There are very few reports claiming the isomorphous substitution of Si (or Al) by a doubly charged cation in the framework of an aluminosilicate zeolite. Small amounts of Be^{2+} incorporation into the zeolite ZSM-5 have been reported by direct synthesis (Si/Be > 30)[11] and by postsynthesis treatments (Si/Be = 2280).[12] Unfortunately, in both cases, only ^9Be MAS NMR was used to characterize the isomorphous substitution. A difference of 2.3 ppm in the chemical shift of ^9Be (line broadening of at least 7 ppm) with respect to dense beryllosilicates was used to

---

* To whom correspondence should be addressed.

[†] On leave from Instituto de Tecnologia Quimica, Valencia, Spain.

[®] Abstract published in *Advance ACS Abstracts*, October 15, 1994.

(1) Davis, M. E.; Lobo, R. L. *Chem. Mater.*, **1992**, *4*, 756.

(2) Ueda, S.; Koizumi, M.; Baerlocher, Ch.; McCusker, L. B.; Meier, W. M. *7th IZC* **1986**, Poster Paper 3c-3.

(3) Annen, M. J.; Davis, M. E.; Higgins, J. B.; Schlenker, J. L. *J. Chem. Soc., Chem. Commun.* **1991**, 1175.

(4) Lawton, S. L.; Rohrbaugh, W. J. *Science* **1990**, *247*, 1319.

(5) Brunner, G. O.; Meier, W. M. *Nature* **1989**, *337*, 146.

(6) Harrison, W. T. A.; Nenoff, T. M.; Eddy, M. M.; Martin, T. E.; Stucky, G. E. *J. Mater. Chem.* **1992**, *2*, 1127.

(7) Harrison, W. T. A.; Gier, T. E.; Stucky, G. D. *J. Mater. Chem.* **1991**, *1*, 153.

(8) Camblor, M. A.; Davis, M. E., manuscript in preparation.

(9) Annen, M. J. Ph.D. Thesis, Virginia Polytechnic Institute and State University, 1992.

(10) Annen, M. J.; Davis, M. E. *Microporous Mater.* **1993**, *1*, 57.

(11) Romannikov, V. N.; Chumachenko, L. S.; Mastikhin, V. M.; Ione, K. G. *J. Catal.* **1985**, *94*, 508.

(12) Han, S.; Schmitt, K. D.; Shihabi, D. S.; Chang, C. D. *J. Chem. Soc., Chem. Commun.* **1993**, 1287.

0897-4756/94/2806-2193$04.50/0

demonstrate the incorporation of Be into framework positions of the zeolite. Additionally, Rossin *et al.* showed that Co^{2+} could reside in framework positions of ZSM-5.[13] As with Be^{2+}, the extent of substitution was very low, Si/Co ~ 200.

We present here the first example of extensive isomorphous substitution of Si (Al) by a large divalent element (Zn^{2+}) in the framework of a relatively low FD (ca. 17 T/1000 $Å^3$) silica-based zeolite: Zn−SOD. The charge introduced in the SOD framework by Zn^{2+} is counterbalanced by the organic structure-directing molecule, tetramethylammonium (TMA^+) and by Na^+. Thus, the feasibility of "templating" low FD, silica-based solids with Zn^{2+} in framework positions and the extensive substitution of Zn^{2+} for Al^{3+} in relatively low-silica zeolites is demonstrated.

Experimental Section

Zn−SOD samples were synthesized in Teflon-lined stainless steel Parr bombs heated statically for 2 weeks at 150 °C. Chemical reagents used included TMAOH (25 wt % aqueous solution, Johnson-Matthey), TMACl (97%, Aldrich), (TMA-d_{12})-$OD{\cdot}5D_2O$ (Cambridge Isotope Labs), zinc acetate dihydrate (Fisher), NaOH (97%, EM), NaCl (EM), silica sol (HS-40, DuPont), and distilled water. Starting mixtures of composition $0.18Na(OH,Cl){:}0.78TMA(OH,Cl){:}0.03Zn(CH_3COO)_2{:}SiO_2{:}21H_2O$ with Cl^-/OH^- ratios of 0 and 0.78 were prepared in order to crystallize pure Zn−SOD. For the latter case, NaCl and a mixture of TMACl and TMAOH were used to fix the Cl^-/OH^- ratio to 0.78. Si/Zn ratios lower than 33 led to mixtures of VPI-7 and zincosilicate SOD while higher Cl^-/OH^- ratios (1.5) yielded amorphous solids even after 7 weeks of heating at the crystallization temperature. If the reaction mixtures are heated at 175 °C, Zn−SOD can be obtained in approximately 5 days. Upon quenching the bombs and recovering the solid product by filtration, the samples were exhaustively washed with water and dried at around 60 °C.

Crystallinity and phase purity of the solids were determined by X-ray powder diffraction using a Scintag XDS-2000 diffractometer (Cu Kα radiation). The unit-cell parameters were refined by a least-squares method using fluorophlogopite as an internal standard. A synchrotron XRD pattern of one of the samples was recorded in the 2θ range of 10−75° at the Brookhaven National Laboratory using a wavelength of 1.299 34 Å.

Thermogravimetric analyses (TGA) and differential thermal analyses (DTA) were performed in air at a heating rate of 10 °C/min on a DuPont 951 thermogravimetric analyzer and a Dupont 910 differential thermal analyzer, respectively. Chemical analyses for Si, Zn, and Na were obtained from Galbraith Laboratories. C, H, and N elemental analyses were performed at Chevron Research Laboratories in Richmond, CA.

^{29}Si MAS NMR and $^{13}C-^1H$-decoupled MAS NMR spectra were collected on a Bruker AM-300 spectrometer at a spinning rate of 4 kHz using 7 mm rotors and were referenced to tetrakis(trimethylsilyl)silane (downfield resonance at −10.05 ppm relative to TMS) and adamantane (down field resonance at 38.4 ppm), respectively, and the results are reported referenced to TMS. ^1H and ^{23}Na MAS NMR spectra were measured on the same spectrometer at 7.0 T in 4 mm rotors at a spinning rate of 8 kHz. The chemical shifts are reported relative to TMS and solid NaCl, respectively. For ^{23}Na, the flip angle (determined on the reference sample) did not exceed $\pi/8$ in order to get a uniform excitation of the spin−3/2 nucleus. Product Si/Zn ratios were calculated from ^{29}Si MAS NMR spectra using the Bruker LINESIM Gaussian-fitting software. IR spectra were recorded on a Nicolet FTIR 800 spectrometer using the KBr pellet technique.

Results and Discussion

A zincosilicate with the SOD structure is synthesized at hydrothermal conditions for the first time. The Cl^-/OH^- ratio of the starting mixture (0 and 0.78) has a strong influence on the chemical composition of the crystallization product, although all samples show XRD patterns typical of the SOD topology. Cl^-/OH^- ratios of 0 and 0.78 yield pure Zn−SOD with high and low Zn contents, respectively. Hereinafter, these materials will be denoted as h-Zn−SOD-50 (Si/Zn = 6.5, synthesized at 150 °C), h-Zn−SOD-75 (Si/Zn = 6.2, synthesized at 175 °C) and l-Zn−SOD (Si/Zn = 12.8, synthesized at 150 °C). Analogous to aluminum incorporation in zeolites, the greater amount of Zn substitution for silicon occurs at the higher pH (Cl^-/OH = 0). From the yield of solids and their chemical composition (vide infra), approximately 97% and 86% of the Zn present in the starting mixture is incorporated to the SOD framework in the synthesis of h-Zn−SOD-50 and l-Zn−SOD, respectively. Zn is thus the limiting element in the synthesis. This is not surprising since pure-silica SOD is not expected to crystallize when using TMA^+ as the structure-directing agent. The crystallization of Zn−SOD occurs in the presence of Na^+ which has been previously shown to strongly direct the hydrothermal synthesis of VPI-7 over a wide range of synthesis conditions.[9,14] Most likely, the high TMA^+/Na^+ ratios used here (4.3, compared to $TMA/(Na^+ + K^+)$ ~ 0.07 that is typical for the synthesis of VPI-7[9]) favor the nucleation of Zn−SOD over VPI-7.

The XRD patterns of h-Zn−SOD and l-Zn−SOD reveal that all the materials are highly crystalline and no indication of impurity phases are detected. h-Zn−SOD shows much narrower XRD peaks than l-Zn−SOD. The difference in peak widths is attributed to the size of the crystals. SEM results reveal that the h-Zn−SOD crystals have cubic morphology with edges of about 2 μm in length, whereas l-Zn−SOD appears as spherulites (most likely aggregates of much smaller crystals) with diameters ranging from about 0.5 to 1.5 μm. The synchrotron XRD pattern of h-Zn−SOD-50 is shown in Figure 1. The XRD patterns of the Zn−SOD materials have been indexed to a cubic unit cell and the decrease in unit cell size for l-Zn−SOD relative to h-Zn−SOD is consistent with their Si/Zn ratios (see Table 1). The XRD patterns from h-Zn−SOD and l-Zn−SOD display the same reflections found in the TMA^+-containing aluminosilicate,[15] ferrisilicate,[16] and gallosilicate[17] analogues and in the (ethylene glycol-containing) pure-silica SOD,[18] although the exact 2θ positions vary in all these materials because of the unit-cell size variations due to the sizes of Zn^{2+} (0.83 Å), Al^{3+} (0.57 Å), Fe^{3+} (0.67 Å), and Ga^{3+} (0.62 Å). An indication of the isomorphous substitution of Si by the aforementioned cations in the SOD framework is reflected in the unit-cell parameters listed in Table 1. Although the unit-cell parameters are expected to depend also on the nature and size of the inorganic and/or organic substances entrapped in the

---

[13] Rossin, J. A.; Saldarriaga, C.; Davis, M. E. *Zeolites* **1987**, *7*, 295.

[14] Annen, M. J.; Davis, M. E. *Synthesis of Microporous Materials*, Van Nostrand Reinhold, New York, 1992; Vol. I. p 340.

[15] Baerlocher, Ch.; Meier, W. M. *Helv. Chim. Acta* **1969**, *52*, 1853.

[16] Szostak, R.; Thomas, T. L. *J. Chem. Soc., Chem. Commun.* **1986**, 113.

[17] Lortz, W.; Schön, G. *J. Chem. Soc., Dalton Trans.* **1987**, 623.

[18] Richardson, Jr., J. W.; Pluth, J. J.; Smith, J. V.; Dytrych, W. J.; Bibby, D. M. *J. Phys. Chem.* **1988**, *92*, 243.

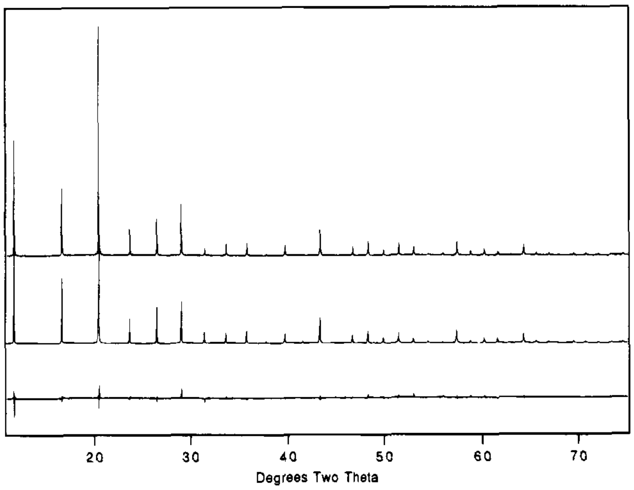

Figure 1. Experimental (top) and simulated (middle) synchrotron X-ray powder diffraction patterns of h-Zn–SOD-50 (λ=1.299 34 Å). The bottom trace is the difference between the top and middle patterns.

Table 1. Unit-Cell Parameter for Cubic SOD Phases

	a (Å)	V (Å^3)	Si/T^c	ref
(TMA,Na)–Zn,Si–SOD (h-50)	8.976^a	723	6.5	this work
	8.975^b	723	6.5	this work
(TMA,Na)–Zn,Si–SOD (l)	8.954	718	12.8	this work
($C_2H_6O_2$)–Si–SOD	8.830	692	–	18
(TMA,Na)–Al,Si–SOD	8.968	721	4	16
(TMA)–Fe,Si–SOD	9.001	729	5.5	16
(TMA)–Ga,Si–SOD	8.925	711	5	17

^{a} Cu Kα radiation. ^{b} Synchrotron radiation. ^{c} Molar ratio of Si to the heteroatom T.

sodalite cages (β cage) the TMA$^+$-containing sodalites (Fe, Al, Ga, and Zn analogues) can be directly compared.

Thermogravimetric analyses from the Zn–SOD samples are shown in Figure 2. According to differential thermal analyses (not shown), two exothermic processes occur at temperatures above 670 and 920 K, respectively. The exact assignments of these weight losses are difficult without further information, e.g., on-line mass spectroscopy. However, one description that gives results that compare favorably with bulk elemental-analyses is as follows. The weight loss below ~670 K is assigned to the desorption of H_2O. Dehydration of l-Zn–SOD occurs in two steps (up to ~420 K and between 420 and 650 K). At temperatures above 670 K (l-Zn–SOD) or 720 K (h-Zn–SOD) combustion and pyrolysis of the TMA$^+$ molecules occur. At even higher temperatures, carbonaceous residues from the TMA$^+$ pyrolysis are oxidized and removed as carbon oxides. The last step is more evident and begins at higher temperature in the sample with higher Zn content: ~1020 K in h-Zn–SOD compared to ~920 K in l-Zn–SOD (according to DTA). This effect is partially due to the smaller crystal size of l-Zn–SOD. Total collapse of the SOD structure occurs during these processes (yielding a XRD pattern indicative of a dense material), and even after calcination in air at 1125 K, some carbonaceous residue still remains in the solid. $^{13}C-^{1}H$-decoupled MAS NMR of as-made Zn–SOD (not shown) gives a single line centered at 58.0 ppm in agreement with the results reported for TMA–Al-SOD.[19] Thus, TMA$^+$ cations are encapsulated intact in the β-cages. Knowing that TMA$^+$ is intact, the assignments of the TGA weight losses give TMA$^+$ contents that agree reasonably well with the results of C, H, N analyses (see Table 2).

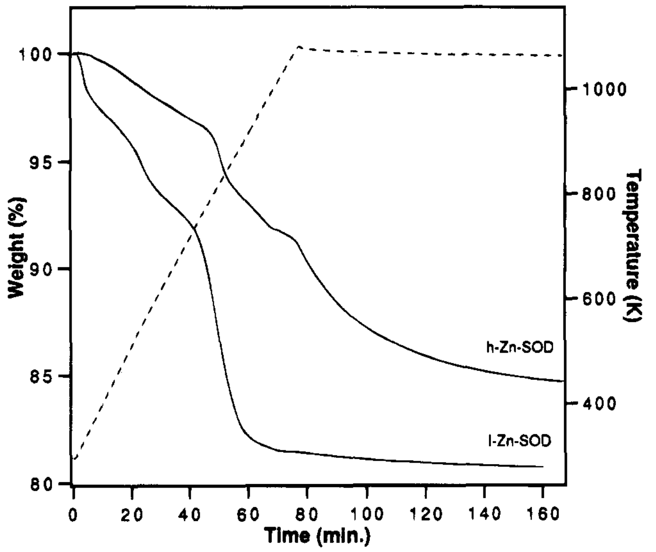

Figure 2. TGA data of Zn–SOD samples (solid lines). The dashed line is for the temperature. h-Zn–SOD-50 and h-Zn–SOD-75 (not shown) reveal similar TGA patterns.

Chemical analyses of Si, Zn, and Na (Table 2) when used with the TGA results and the C, H, N elemental analyses give the following cubic unit cell compositions: $TMA_{1.5}Na_{2.1}[Zn_{1.6}Si_{10.4}O_{24}](X)_{0.4}$ for h-Zn–SOD-50, $TMA_{1.4}Na_{2.4}[Zn_{1.7}Si_{10.3}O_{24}](X)_{0.4}$ for h-Zn–SOD-75 and $TMA_{1.5}Na_{0.8}[Zn_{0.9}Si_{11.1}O_{24}](X)_{0.5}$ for l-Zn–SOD, where X denotes an anion. Because no care was taken to expose the samples to a specific relative humidity, the water contents measured by TGA must be interpreted with care. Thus, the compositions are written on an anhydrous basis. Note that for h-Zn–SOD and l-Zn–SOD it is necessary to place anions, e.g., could be OH^- (or Cl^- with l-Zn–SOD), in the composition for charge balancing (recall that two charges are created by the substitution of Zn^{2+} for Si^{4+}). However, the added anion charge is relatively small and could be zero if uncertainties in the chemical analyses are considered. Therefore, it is not clear from chemical analysis whether occluded anions are present in Zn–SOD or not. For aluminosilicate sodalites $(Na_{3+x}(OH)_x{\cdot}nH_2O)_2[SiAlO_4]_6$ there can be three sodium cations and not more than four water molecules per sodalite cage (nonbasic hydrosodalite: $x = 0$, $n \leq 4$), or for the basic hydrosodalite four sodium cations, one OH^- anion, and one or no H_2O molecule per cage ($x = 1$, $n = 1$ or 0).[20] The ^{1}H and ^{23}Na MAS NMR spectra of the aluminosilicate materials differ significantly.[20] Thus, we performed ^{1}H and ^{23}Na NMR studies on h-Zn–SOD. The ^{1}H MAS NMR spectrum of h-Zn–SOD-containing deuterated TMA$^+$ is shown in Figure 3a. ((TMA-d_{12})OD·5D_2O was used in this sample of h-Zn–SOD in order to decrease the large ^{1}H signal from TMA$^+$.) Besides a peak at 3.2 ppm arising from residual protons in the deuterated TMA$^+$, a signal at 4.6 ppm appears which is similar to that one in the ^{1}H MAS NMR spectrum of the nonbasic hydrosodalite

---

(19) Jarman, R. H.; Melchior, M. T. *J. Chem. Soc., Chem. Commun.* **1984**, 414.

(20) Engelhardt, G.; Felsche, J.; Sieger, P. *J. Am. Chem. Soc.* **1992**, *114*, 1173.

Table 2. Compositions of Zn–SOD

	chemical analysis		C, H, N analysis			TGA[c]	
sample	Si/Zn[a]	Na/Zn[a]	C/N[a]	H/C[a]	total[b]	H_2O[b]	TMA[b]
h-Zn–SOD-50	6.5	1.3	4.2	3.8	12.7	3.4 (<670)	13.2 (>720)
h-ZN–SOD-75	6.2	1.4				6.0 (<670)	12.6 (>720)
l-Zn–SOD	12.8	0.9	4.3	3.5	15.6	3.7 (<420) 5.2 (420–670)	14.5 (>670)

[a] Molar ratios. [b] g per 100 g of calcined solid. [c] See text for TGA assignments. Temperature limits in kelvin are given in parentheses.

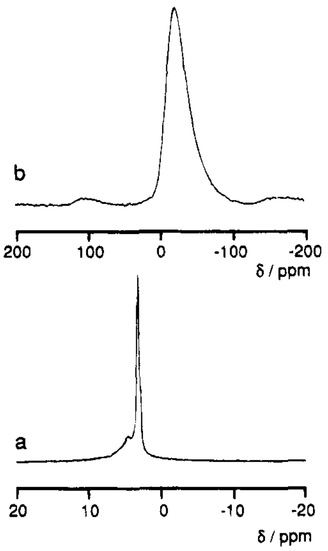

Figure 3. ^1H (a) and ^{23}Na (b) MAS NMR spectra of h-Zn–SOD-75 synthesized with $(TMA\text{-}d_{12})OD{\cdot}5D_2O$.

$(Na_3(H_2O)_4)_2[SiAlO_4]_6$. Additionally, this chemical shift resembles those of H_2O in liquid water and in other zeolites.[21] No lines like those reported from the basic hydrosodalites[20] at 16.3 and −0.1 ppm ($H_3O_2^-$) and −3.8 ppm (OH^-) are observed. From the ^1H MAS NMR spectrum in Figure 3a it thus follows that the cages are either filled with Na^+ cations and H_2O molecules or with TMA^+ cations considering that cages with TMA^+ cannot contain anything else.

Unlike the protons discussed above, the sodium cations interact with the sodalite framework because they are coordinated to framework oxygen atoms. The ^{23}Na MAS NMR spectrum of zinc sodalites may therefore be different from those of aluminosilicate sodalites due to the different framework compositions. This is manifested in the ^{23}Na MAS NMR spectrum of h-Zn–SOD in Figure 3b where a broad unsymmetrical line at ca. −19 ppm is shown and is different from all known aluminosilicate hydrosodalites.[20] However, due to the different magnetic field strengths used for the ^{23}Na MAS NMR spectra of the nonbasic hydrosodalite $(Na_3(H_2O)_4)_2[SiAlO_4]_6$ or the basic hydrosodalite $(Na_4H_3O_2)_2[SiAlO_4]_6$ in ref 20 and the spectrum shown in Figure 3b, it cannot be excluded that quadrupolar interaction is responsible for the difference. Without further ^{23}Na NMR studies of Zn–SOD at different magnetic fields it cannot be ascertained if there is a similarity between the ^{23}Na MAS NMR spectra of h-Zn–SOD and aluminosilicate sodalites. It should be mentioned that washing of the products did not affect the ^{23}Na MAS NMR spectra of h-Zn–SOD unlike the basic hydrosodalite $(Na_4H_3O_2)_2[SiAlO_4]_6$ which crystallizes at highly basic conditions.

The results from chemical analyses and the ^1H and ^{23}Na MAS NMR spectroscopies reveal that h-Zn–SOD contains two types of cage fillings, TMA^+ or Na^+ ions. Since there are two β-cages per unit cell,[22] the anhydrous, *ideal* composition of h-Zn–SOD can be written as

$$[TMA^+]_{1.4}\cdot[Na_3^{3+}]_{0.6}\cdot[Zn_{1.6}Si_{10.4}O_{24}]$$

Although the compositions of the Zn–SOD samples are written as a combination of the TMA^+– and Na_3^{3+} Zn–SOD ideal end members, the XRD patterns suggest that these materials are neither intergrowths or physical mixtures of these end members. As stated above, all XRD patterns index perfectly to a cubic unit cell of about 9 Å . Moreover, the synchrotron XRD pattern shows very narrow and symmetric peaks with no indication of splittings in the measured 2θ range (Figure 1). This pattern is indexed to a cubic unit cell with $a = 8.975$ Å and systematic absences indicative of a body-centered cell. It is most likely that in Zn–SOD there is no long-range order of Zn and Si in framework positions and of $[TMA]^+$ and Na^+ ions among the β-cages.

From the chemical composition shown in Table 2, it can be seen that despite the large cationic radius of Zn^{2+} and the necessity of counterbalancing two negative charges per ZnO_4^{2-} unit, the extensive isomorphous substitution of Zn for Si (Al) can be obtained in the SOD framework. Additionally, the void spaces in the crystalline zincosilicate framework can be occupied by the relatively voluminous cation TMA^+. These results are better understood by realizing that in the SOD topology, all the tetrahedral framework atoms face four sodalite cavities (β-cages). This allows for an effective counterbalancing by TMA^+ (and Na^+) on all sides of the ZnO_4^{2-} unit. Also, note that the h-Zn–SOD sample has a higher framework negative charge density (0.27 charges/T atom) than other reported TMA^+-containing SOD materials: Al–(0.2), Ga–(0.17), and Fe–(0.15) (values calculated from the smaller Si-to-heteroatom ratios reported: 4,[16] 5,[17] and 5.5[16] for the Al, Ga, and Fe analogues, respectively).

IR spectroscopy in the region of framework vibrations provides a clear indication of the isomorphous substitution as the position of the intense TOT asymmetric stretching band appearing around 1000 cm^{-1} is shifted about 18 cm^{-1} to lower wavenumbers (h-Zn–SOD, Si/Zn = 6.5, $\nu_{TOT} = 1062\ cm^{-1}$) relative to TMA–Al–SOD (Si/Al = 5, $\nu_{TOT} = 1080\ cm^{-1}$).[17] This is a consequence of the much larger Zn–O bond distance (~1.95 Å) when compared to the Al–O (1.77 Å) and Si–O (1.60 Å) bond distances. For l-Zn–SOD, $\nu_{TOT} = 1073\ cm^{-1}$ in good agreement with its lower Zn content.

---

(21) Pfeifer, H.; Freude, D.; Hunger, M. *Zeolites* **1985**, *5*, 234.

(22) Meier, W. M.; Olson, D. H. *Atlas of Zeolite Structure Types*, 3rd ed.; Butterworth-Heinemann: London 1992.

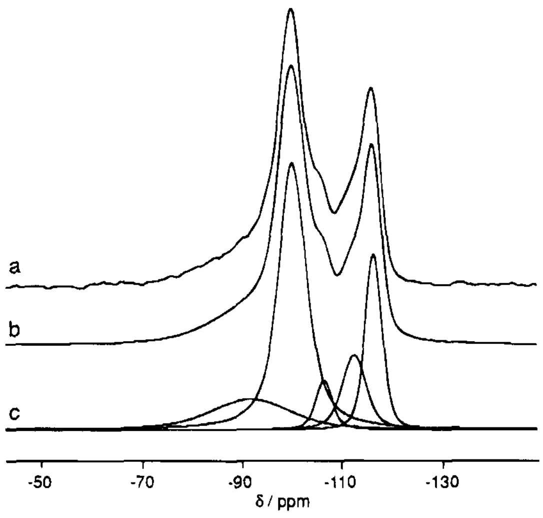

Figure 4. ^{29}Si MAS NMR of h-Zn–SOD-75 (a), the simulated spectrum (b), and the deconvoluted components of the spectrum (c).

Table 3. Chemical Shifts, Relative Intensities, and Assignments of the ^{29}Si NMR Peaks of Zn–SOD Phases

ppm (from TMS)	area %	assignment	$(Si/Zn)_{NMR}$	$(Si/Zn)_{chem\ anal.}$
		h-Zn–SOD-75		
−116.4	17.8	Si(0Zn)		
−112.5	11.3	Si(0Zn)		
−106.5	5.2	Si(0Zn)	6.2	6.2
−100.2	50.5	Si(1Zn)		
−91.7	15.2	Si(1Zn)		
		l-Zn–SOD		
−116.2	25.6	Si(0Zn)		
−112.3	21.0	Si(0Zn)		
−104.9	22.0	Si(0Zn)	12.7	12.8
−100.3	19.0	Si(1Zn)		
−96.1	12.4	Si(1Zn)		

The ^{29}Si MAS NMR spectrum of h-Zn–SOD is shown in Figure 4 together with the simulation and its components. Additionally the results from the spectral deconvolution and the assignment of the peaks are listed in Table 3. The line assignments given in Table 3 are somewhat tentative; however, any other combinations give Si/Zn ratios *lower* than obtained from bulk elemental analysis. The presence of amorphous impurities which could affect the results can be excluded on the basis of the X-ray diffraction experiments and SEM photographs. An attempt to interpret the ^{29}Si MAS NMR spectra of zinc sodalites and to justify the line assignments in Table 3 is given below.

The ^{29}Si MAS NMR spectrum of h-Zn–SOD is discussed in detail here; however, the conclusions can in principle also be applied to l-Zn–SOD. Assuming a random distribution for Zn, the expected line intensities for Si with no Zn in the first T-atom coordination shell, Si(0Zn), for Si with one Zn in the first T-atom coordination shell, Si(1Zn), etc., can be calculated.[23] For a Si/Zn ratio of 6.2, the expected line intensities are 50% for Si(0Zn), 38% for Si(1Zn), 11% for Si(2Zn), 1% for 3(Zn), and less than 1% for Si(4Zn). A preliminary study by Camblor and Davis on ^{29}Si NMR chemical shifts in zincosilicates has shown that the effect of a Zn atom neighboring a silicon atom on the ^{29}Si chemical shift is very large.[24] According to these results, the strongest peak at −100.2 ppm in Figure 4 has to be assigned unambiguously to Si(1Zn). The intensity of this line is 50.2%, i.e., it is significantly higher than expected from a random distribution of Zn. On the other hand, if it is tentatively assumed that all three lines at −116.4, −112.5, and −106.5 ppm represent Si(0Zn), the overall intensity of these three lines (34.3%) is lower than expected from random Zn distribution. It follows that this deviation of the line intensities of Si(0Zn) and Si(1Zn) from a random distribution of Zn atoms must be accompanied by a lower concentration of Si(2Zn), Si(3Zn), and Si(4Zn) in order to maintain the overall Si/Zn ratio and thus they do not occur at all. These observations can be rationalized in terms of the repulsion between the charges introduced into the framework by the Zn atoms which induces a nonrandom distribution of Zn atoms in the *local* silicon coordination in order to increase the average distance between Zn atoms in the sodalite framework. However, there must be a lack of translational symmetry of this nonrandom distribution, since no long-range order is observed in the X-ray diffraction experiments. The lack of long-range heteroatom ordering is also present in the TMA$^+$ aluminosilicate SOD.[15] In this sense, the distribution of the Zn atoms in the sodalite framework may be nonrandom in a local sense but disordered over the long range probed by XRD.

Since more than two lines are observed in the ^{29}Si MAS NMR spectra of the Zn–sodalite samples, effects other than the atom distribution in the first T-atom shell coordination must play a role in determining the ^{29}Si chemical shielding. The occurrence of different crystallographic sites can be excluded on the basis of the cubic symmetry of the materials. A possible explanation could be the effect of the second T-atom shell coordination. Due to the large difference in chemical shift of 16.2 ppm between the two main peaks at −116.4 and −100.2 ppm for a difference of one Zn in the first T-atom coordination shell, it seems reasonable that smaller but observable differences occur for the second shell T-atom distribution. Much smaller second shell effects are also suspected in the ^{29}Si MAS NMR spectra of aluminosilicates,[25] and it has to be emphasized that the influence of aluminum in the first shell (ca. 5 ppm) is much smaller than that of zinc (ca. 16 ppm). Accordingly, the line multiplicities may be assigned to second-shell coordination T-atom ordering; however, the number of Zn atoms in the second shell cannot be solely ascertained by the ^{29}Si MAS NMR data given in this paper. Another explanation for the additional lines could be an effect of the different cage fillings. However, for aluminosilicate sodalites Engelhardt *et al.* have shown that this will only happen when segregated phase domains exist[26] (not observed in the X-ray diffraction patterns of the Zn–SOD samples). Additionally, it may make a difference if a zinc atom in the first or second shell next to a silicon atom is in a four ring or in a six ring of the sodalite framework which could create different distortions of the T–O–T angles. A conclusive interpretation of the observed line splittings in the ^{29}Si

---

[23] Engelhardt, G.; Michel, D. *High Resolution Solid-State NMR of Silicates and Zeolites*; Wiley: Chichester, 1989.

[24] Camblor, M. A.; Davis, M. E., submitted to *J. Phys. Chem.*

[25] Fyfe, C. A.; Gobby, G. C.; Murphy, W. J.; Ozubko, R. S.; Slack, D. A. *J. Amer. Chem. Soc.* **1984**, *106*, 4435.

[26] Engelhardt, G.; Sieger, P.; Felsche J. *Anal. Chim. Acta*, **1993**, *283*, 967.

Table 4. Crystallographic Data for h-Zn–SOD-50

data collection temp	298 K
wavelength	1.2993 Å
profile range	11–75°
step scan increment	0.01
space group	$I\bar{4}3m$ (217)
a	8.9751(2) Å
no. of observations	6401
no. of reflections	46
no. of uniquely defined reflections	23
no. of profile parameters	8
no. of structural parameters	10
R_{wp}	13.1%
R_p	10.5%

Table 5. Atomic Positional Parameters and Isotropic Displacement Parameters (Å^2)[a]

atom	occupancy	site	x	y	z	U
Si	0.867	12d	1/4	1/2	0	0.014[b]
Zn	0.133	12d	1/4	1/2	0	0.014[b]
O(1)	1	24g	0.1512(2)	0.1512(2)	0.4776(8)	0.042
N	0.70[c]	2a	0	0	0	0.022
C(1a)	0.35[c]	8c	0.0947(3)	0.0947(3)	0.0947(3)	0.10[d]
C(1b)	0.35[c]	8c	−0.0947(3)	0.0947(3)	0.0947(3)	0.10[d]
Na(1a)	0.1125	8c	0.162(2)	0.162(2)	0.162(2)	0.04[e]
Na(1b)	0.1125	8c	−0.162(2)	0.162(2)	0.162(2)	0.04[e]
O(2a)	0.15	8c	0.090(1)	0.090(1)	0.090(1)	0.05[e]
O(2b)	0.15	8c	0.090(1)	0.090(1)	0.090(1)	0.05[e]

[a] The atomic positional parameters of atoms labeled a and b were related by a mirror plane, i.e., do not involve more variable parameters. This was done to partially account for the disorder of the occluded atoms. Occupancy factors were not optimized. See text. [b] Refined as one variable. [c] C/N ratio was constrained to a ratio of 4. [d] Refined as one variable. [e] These temperature factors were not refined, from ref. 29.

Table 6. Selected Bond Distances (Å) and Angles (deg) and Their Esd's in Parentheses

	h-Zn–SOD-50
Si(Zn)–O	1.634(1)
O–Si(Zn)–O	114.3 (2), 107.1 (1)
Si(Zn)–O–Si(Zn)	152.4 (3)
N–C	1.47 (1)
O(1)–Na(1a)	2.84 (1)
O(1)–Na(b)	2.68 (1)
Na(1a)–O(2b)	2.43 (2)
Na(1b)–O(2a)	2.43 (2)
Na(1a)–Na(1a)	4.10 (3)

MAS NMR spectra of zinc sodalites is still lacking, and this requires further investigation which is beyond the scope of this paper.

To gain further confidence in the conclusions made thus far, a Rietveld refinement was performed on the XRD data collected from h-Zn–SOD-50. The XRD pattern was initially indexed with lattice parameter a = 8.97 Å, and systematic absences were in agreement with a body-centered space group. The maximum topological symmetry of the sodalite framework is $Im3m$. However, the framework normally adapts to the size and shape of the ions occluded inside the β-cages, which normally lowers the symmetry of the material. The refinement was initiated using the space group $I\bar{4}3m$, which is the highest possible symmetry of a partially deformed sodalite framework.[27]

The General Structure Analysis Program[28] (GSAS) was used for the refinement of h–Zn–SOD. The crystallographic data for the refinement are summarized in Table 4. Initially, only the framework atoms were included in the refinement and the Si/Zn ratio was constrained to a ratio of 6.5. No geometric constraints were used during this stage of the refinement. Therefore the effect of the isomorphous substitution of Zn in the framework was modeled as partial occupancies of Zn in the T-atom positions (see Table 5). The use of fractional occupancies for Zn in the T-atom positions does not account for the local distortion of T–O bonds and angles produced by the Zn; given the relatively small number of observed reflections, more complex models would contain too many variable parameters in the refinement. Inspection of the difference Fourier map indicated the presence of the TMA molecules inside the β-cages. ^{1}H and ^{13}C MAS NMR spectroscopies of the sample (*vide supra*) show that the TMA molecule—on the NMR time scale—is very mobile inside the sodalite cages. This disorder was partially simulated in the refinement by placing the TMA molecule in two different configurations (C(1a) and C(1b) in Table 5). With both of these configurations, the N–C bond is parallel to the ⟨111⟩ directions and the C atoms effectively form a cube around the N atoms (see Table 5). The C/N ratio was constrained to 4 and left as such throughout the refinement. During this stage of the refinement the occupancies of the N and C atoms were kept constant at 0.7 TMA$^+$ cations per cage in accordance with the bulk chemical analysis. No geometric constrains were forced on the C–N bond length.

Further difference Fourier maps showed the presence of missing electron density near the positions where Na$^+$ cations are observed in aluminosilicate sodalites.[29] However, because of the higher symmetry of the $I\bar{4}3m$ space group of this material compared to the $P\bar{4}3n$ which was used for the aluminosilicate sodalites, there are eight possible positions for the sodium cations per cage. This implies that on average the sodium cations are disordered over these two positions. Because more than half of the β-cages are filled with TMA cations, no correlation is expected between the configuration of different Na-containing cages. This is in contrast to the aluminosilicate sodalites in which the Na clusters are related by an n-glide. A new difference Fourier map only showed missing electron density between the Na cations and the C atoms of the TMA, but no clear maxima were observed that indicated the positions of missing atoms. This effect is probably the result of the combination of the scattering from the H atoms from TMA (on average about 9 electrons/cage) and water molecules coordinated to the Na cations. It was decided to use first O atoms in the expected positions for coordination to Na$^+$, also disordered as in the case of Na$^+$.

In the final refinement (Figure 1, R_p of 10.5%), all atomic coordinates and thermal parameters were refined. Table 5 shows the results and indicates the constraints used during the final refinement. Almost no improvement was observed in the R_p factor if the H atoms of the TMA were included in the refinement (were left out of the final model).

The Rietveld refinement of the Zn–SOD gives Si(Zn)–O bond distances (Table 6) in agreement with the

---

(27) Depmeier, W. *Acta Crystallogr.* **1984**, *C40*, 226.

(28) Larson, A. C.; Von Dreele, R. B., General Structures Analysis System, LANSCE, Los Alamos National Laboratory, Los Alamos, NM, 1990.

(29) Felsche, J.; Luger, S.; Baerlocher, Ch. *Zeolites* **1986**, *6*, 367.

expected average values ($1.6 \times 0.87 + 1.9 \times 0.13 = 1.647$ Å). C−N bond distances are in very good agreement with the expected values. The long C−O distances (over 3 Å, see Table 6) suggest that there is plenty of space inside the sodalite cage for the molecule to rotate as concluded from the ^{1}H and ^{13}C MAS NMR spectroscopies. The large thermal parameters for the C atoms (0.1 Å^2) are a consequence of this dynamic character of the TMA cations inside the cages. Na^+ framework oxygen (O(1)) and Na^+ oxygen (from water) distances are in reasonable agreement with the values reported for sodium sodalite.[29] If fractional occupancies of water molecules and Na^+ cations were optimized, they would converge to values not in agreement with the chemical analysis, with very little improvement in the values of the residuals (R_p of 10.2%). Because of this, the occupancies were left constant in the final refinement. We consider that this disagreement reflects some of the limitations of the Rietveld methodology for the refinement of crystal structures. In addition to the small number of uniquely defined reflections present in the XRD pattern (23 reflections for a total of 10 structural parameters), sodium and water are found only in 30% of the sodalite cages (from chemical analysis) and constitute a minor fraction of all the scattering atoms in the crystal. Also, the disorder presented by the TMA inside the sodalite cages and the probable orientational disorder of the sodium and water molecules occluded in the cages reduce the effectiveness of the Rietveld refinement method for structure analysis. In a sense, the structure of Zn−SOD can be viewed as a glass within a crystalline framework; that is, despite the local distortions created by the isomorphous substitution of Zn for Si, the four−connected framework shows a high degree of order. In contrast, the ions and molecules found inside the cages show a relatively low long range order probably created by the relatively week interactions between the material occluded inside the cages, and the mostly silica framework.

A detailed structural characterization of h-Zn−SOD requires more information than what can be gathered from the X-ray powder method. The structural model that has been refined here is an approximation of the actual structure of this complicated material. The model however, confirms the isomorphous substitution of Zn^{2+} for Si^{4+} in the sodalite framework, as well as the presence of TMA^+ and Na^+ cations inside the sodalite cages.

The existence of Zn−SOD and in particular h-Zn−SOD shows that high levels of zinc substitution can occur in zeolite frameworks. Although the zinc incorporation is conclusively proven here, there are numerous unanswered questions concerning the details of the local bonding and structure of the framework Zn sites. The Zn−SOD materials can serve as models for understanding the isomorphous substitution of Zn^{2+} into silicate frameworks since other heteroatom substitutions in SOD are known and provide a basis for comparison.

Acknowledgment. Support for this work was provided by the NSF Alan T. Waterman Award to M.E.D. We acknowledge D. E. Cox for assistance in collecting the synchrotron data. The XRD data were collected at X7A beam line, National Synchrotron Light Source, Brookhaven National Laboratory, which is supported by the Department of Energy, Division of Material Sciences and Division of Chemical Sciences. We thank Dr. S. Zones (Chevron) for the C, H, N analyses and Dr. J. Higgins (Mobil) for collecting the synchrotron XRD pattern. M.A.C. gratefully acknowledges the Spanish Ministry of Science and Education and the Fulbright Commission for a postdoctoral fellowship, and the Instituto de Tecnologia Quimica (Valencia, Spain) for permission to leave.